REPORT NO.
UCB/SEMM-91/04

STRUCTURAL ENGINEERING,
MECHANICS AND MATERIALS

3-NODE TRIANGULAR ELEMENTS BASED ON REISSNER-MINDLIN PLATE THEORY

by

FERDINANDO AURICCHIO

and

ROBERT L. TAYLOR

MAY 1991

DEPARTMENT OF CIVIL ENGINEERING
UNIVERSITY OF CALIFORNIA
BERKELEY, CALIFORNIA

THREE NODE TRIANGULAR ELEMENTS BASED ON REISSNER-MINDLIN PLATE THEORY

Ferdinando AURICCHIO and Robert L. TAYLOR

Department of Civil Engineering, University of California at Berkeley, Berkeley, CA 94720, U.S.A.

Contents

Abstract

In this paper we present a finite element algorithm for the solution of plate bending problems which include the primary effects of shearing deformation. A mixed variational formulation is employed to approximate a set of three-node triangular elements. The elements considered possess only the classical three vertex degrees-of-freedom at the global level (i.e., the transverse displacement and two rotations). The mixed patch test is utilized to assess each proposed element for possible shear locking or singularities. Several numerical simulations illustrate the applicability and accuracy of the elements considered.

1. INTRODUCTION

The development of an accurate finite element for the numerical solution of a wide class of plate problems remains a difficult task to perform. A literature on this subject may be found in any standard finite element text (e.g., see [1-3,5]).

Early attempts to develop a viable element were made for the thin Kirchhoff plate theory. Approaching the problem for this theory requires one to assume as nodal degrees of freedom at least the transverse displacement and two rotations at each node. Since the rotations are computed as the derivatives of the transverse displacement, one must use shape functions of class C^1. Also, the implementation of accurate high order elements of this type is usually very complex relative to traditional iso-parametric solid elements [6-8]. Moreover within this theory, transverse shear deformation of the plate is neglected which restricts the range of applications of the theory and sometimes leads to problems in the specification of some simply supported boundary conditions [2-3,5].

In the late sixties attention was devoted to the more general thick, Reissner-Mindlin, plate theory [9-10], in order to avoid all the above difficulties, as well as to extend the range of problems which could be solved by the finite element method. Approaching the problem by this theory not only allows one to take into account transverse shear deformation and to bypass the previous boundary condition problems, but it also permits one to deal with shape functions of class C^0. On the other hand it was discovered quite soon that for the limiting thin plate case gross errors could result in the solution quantities [11]. The problem is a consequence of the energy stored in the transverse shear terms instead of in the bending terms, as required by the thin plate theory. This effect is termed *shear locking* in the finite element literature.

To avoid shear locking several alternatives have been proposed. The first techniques that gave good results were based on (uniform or selective) underintegration of the stiffness matrix; however, sometimes such elements show rank deficiency or zero energy internal mechanisms [12-14]. During the late 1970's, it was discovered that use of selective or reduced integration techniques was equivalent to approaching the problem by a mixed finite element method [15]. This has led to a better understanding of the solution of the plate problem using a finite element method and many new elements were proposed [16-20]. As a consequence of the complexity of the formulation of the problem as contained in the Babuska-Brezzi stability conditions [21-23], many of the new elements were developed more on physical and mechanical intuition than on mathematical considerations.

During the last few years, it has been shown not only that a mixed formulation is the most correct way to approach the plate bending problem, but

that working with a mixed theory also provides additional insight into a wider class of problems involving constraints (e.g., those concerning incompressible media, elastic-perfectly-plastic solids, contact problems, etc.). Thus, mixed procedures provide one with the opportunity to design finite elements capable of good numerical performance for all of the above classes of problems. Moreover some alternative requirements which are much easier to check and involve direct computer solutions or simple algebraic considerations have been shown to be nearly equivalent to the more complex Babuska-Brezzi conditions [24-30].

The purpose of the present paper is to:

(a) briefly review a thick plate theory together with its equivalent variational formulation,

(b) review general mixed finite element approaches for the thick plate theory,

(c) show that high quality interpolating functions for the shear strain and stress fields can be used as well as for the displacement fields,

(d) discuss an existing triangular element and introduce some new simple triangular elements,

(e) illustrate the performance of these elements on some standard test problems.

2. A THICK PLATE THEORY

The term *plate* is used in the present work to denote a flat body in which one dimension, called plate thickness or transverse direction, is much smaller than the other two dimensions. Furthermore, loading is restricted to be applied in the transverse direction only.

Plate theories are commonly classified as *thick* or *thin*. Thick plate theories include both bending deformation and the primary effects of transverse shear whereas thin plate theories include only bending effects. Early development of a thick plate theory are commonly attributed to Reissner [9] and Mindlin [10] and the theory here presented is a simplification of those originally proposed. The basic assumptions, under which the thick plate theory is developed, are:

$$\Omega = \left\{ (x, y, z) \in R^3 \;\middle|\; z \in \left[-\tfrac{1}{2} t \,, +\tfrac{1}{2} t \right], \; (x, y) \in A \subset R^2 \right\} \tag{2.1a}$$

$$\sigma_{zz} = 0 \tag{2.1b}$$

$$u = z\theta_y(x, y) \;, \quad v = -z\theta_x(x, y) \;, \quad w = w(x, y) \tag{2.1c}$$

where u, v and w are the displacements along the x, y and z axes, respectively, and θ_x and θ_y are the small rotations of the transverse line elements about x and y axes. Equation (2.1a) implies that the xy plane for $z=0$ coincides with the mid-surface of the undeformed plate and is merely a geometric definition of the domain occupied by the plate. Equation (2.1b) implies that the normal stress in the z direction is negligible compared to all the other stresses. Although this is inconsistent with a general three-dimensional theory, we can accept it as a consequence of the predominance of the behavior associated with the in-plane two dimensions and as a matter of the fact that it does not influence the development of a viable finite element formulation. The assumption in (2.1b) is not present in the original works by Reissner, where σ_{zz} varies along the thickness. Equation (2.1c) implies that a straight line element, which is normal to the mid-surface of the plate ($z=0$) in the undeformed configuration, remains straight but not necessarily normal to the deformed mid-surface, thus leading to transverse shear deformations. Due to (2.1c) the in-plane displacement u and v can be expressed in terms of the two mid-plane rotations θ_x and θ_y; for this reason the only quantities that determine the displacement fields are w, θ_x and θ_y and so in the following we will refer to them with the general term displacements, without distinguishing between transverse displacement and rotations.

Starting from (2.1), we can divide the strain components into the in-plane bending strains:

$$\varepsilon_x = \frac{\partial u}{\partial x} = z\,\theta_{y,x} \;, \quad \varepsilon_y = \frac{\partial v}{\partial y} = -z\,\theta_{x,y} \tag{2.2a}$$

$$\gamma_{xy} = \frac{\partial u}{\partial y} + \frac{\partial v}{\partial x} = z\left(\theta_{y,y} - \theta_{x,x}\right) \tag{2.2b}$$

and the transverse shear strains:

$$\gamma_{xz} = \frac{\partial u}{\partial z} + \frac{\partial w}{\partial x} = \left(\theta_y + w_{,x}\right) \tag{2.3a}$$

$$\gamma_{yz} = \frac{\partial v}{\partial z} + \frac{\partial w}{\partial y} = \left(-\theta_x + w_{,y}\right) \tag{2.3b}$$

In the thin plate theory the transverse shear strains are assumed to be zero, thus providing constraint equations to replace the θ_x and θ_y rotation components in terms of derivatives of the transverse displacement w. In the thick plate theory this is not possible since shear deformation is considered.

Introducing the hypothesis of an isotropic linear elastic material, for the in-plane stresses the stress-strain relations are:

$$\sigma_x = \frac{E}{1-\nu^2}\left[\varepsilon_x + \nu\,\varepsilon_y\right], \qquad \sigma_y = \frac{E}{1-\nu^2}\left[\varepsilon_y + \nu\,\varepsilon_x\right] \tag{2.4a}$$

$$\sigma_{xy} = G\,\gamma_{xy} \tag{2.4b}$$

and for the transverse stresses are:

$$\sigma_{xz} = G\,\gamma_{xz}, \qquad \sigma_{yz} = G\,\gamma_{yz} \tag{2.5}$$

where E (Young's modulus), ν (Poisson's ratio) and G (shear modulus) are related through the expression:

$$G = \frac{E}{2(1+\nu)} \tag{2.6}$$

Integration of the stresses in the thickness direction permits one to evaluate stress resultants in terms of displacements. If the resultant moments per unit length are defined as:

$$M_x = \int_{-\frac{1}{2}t}^{\frac{1}{2}t} \sigma_x\, z\, dz, \qquad M_y = \int_{-\frac{1}{2}t}^{\frac{1}{2}t} \sigma_y\, z\, dz \tag{2.7a}$$

$$M_{xy} = \int_{-\frac{1}{2}t}^{\frac{1}{2}t} \sigma_{xy}\, z\, dz \tag{2.7b}$$

then from the in-plane stress expressions, we obtain:

$$\mathbf{M} = \mathbf{D}^b\,\mathbf{L}\,\theta \tag{2.8}$$

where

$$\mathbf{M} = \begin{Bmatrix} M_x \\ M_y \\ M_{xy} \end{Bmatrix}, \quad \boldsymbol{\theta} = \begin{Bmatrix} \theta_x \\ \theta_y \end{Bmatrix} \tag{2.9a}$$

$$\mathbf{D}^b = \frac{E t^3}{12(1-\nu^2)} \begin{bmatrix} 1 & \nu & 0 \\ \nu & 1 & 0 \\ 0 & 0 & \frac{1}{2}(1-\nu) \end{bmatrix} \tag{2.9b}$$

and :

$$\mathbf{L} = \begin{bmatrix} 0 & \frac{\partial}{\partial x} \\ -\frac{\partial}{\partial y} & 0 \\ -\frac{\partial}{\partial x} & \frac{\partial}{\partial y} \end{bmatrix} \tag{2.9c}$$

Equation (2.8) can be directly expressed in terms of the curvatures $\boldsymbol{\kappa}$ using the relation:

$$\mathbf{M} = \mathbf{D}^b \boldsymbol{\kappa} \tag{2.10}$$

where:

$$\boldsymbol{\kappa} = \mathbf{L}\boldsymbol{\theta} = \begin{Bmatrix} \theta_{y,x} \\ -\theta_{x,y} \\ \theta_{y,y} - \theta_{x,x} \end{Bmatrix} \tag{2.11}$$

Similarly, defining the resultant transverse shear forces as:

$$S_x = \int_{-\frac{1}{2}t}^{\frac{1}{2}t} \sigma_{xz}\, dz \tag{2.12a}$$

$$S_y = \int_{-\frac{1}{2}t}^{\frac{1}{2}t} \sigma_{yz}\, dz \tag{2.12b}$$

from the transverse stress expressions we obtain:

$$\mathbf{S} = \mathbf{D}^s \boldsymbol{\gamma} \tag{2.13}$$

where

$$\mathbf{S} = \begin{Bmatrix} S_x \\ S_y \end{Bmatrix}, \quad \boldsymbol{\gamma} = \begin{Bmatrix} \gamma_{xz} \\ \gamma_{yz} \end{Bmatrix} = [\mathbf{e}\,\boldsymbol{\theta} + \nabla w] \tag{2.14}$$

and

$$\mathbf{D}^s = kGt \begin{bmatrix} 1 & 0 \\ 0 & 1 \end{bmatrix}, \quad \mathbf{e} = \begin{bmatrix} 0 & 1 \\ -1 & 0 \end{bmatrix} \tag{2.15}$$

where $\mathbf{e}$ is the so called alternating tensor. In $\mathbf{D}^s$, k is a correction factor which depends on the plate properties and for isotropic homogeneous plates is often set equal to 5/6 [9-10,30]. It is introduced to correct the inconsistency with the classical theory due to the transverse shear strain which is constant throughout the thickness as it can be seen from equation (2.3).

Finally, we have to consider transverse linear momentum equilibrium:

$$\nabla^T \mathbf{S} + q = 0 \tag{2.16a}$$

and angular momentum equilibrium about the x and the y axes:

$$\mathbf{L}^T \mathbf{M} + \mathbf{S} = 0 \tag{2.16b}$$

In summary, the complete set of equations governing the thick plate problem may be summarized as:

$$\mathbf{M} = \mathbf{D}^b \boldsymbol{\kappa} \tag{2.17a}$$

$$\mathbf{S} = \mathbf{D}^s \boldsymbol{\gamma} \tag{2.17b}$$

$$\nabla^T \mathbf{S} + q = 0 \tag{2.17c}$$

$$\mathbf{L}^T \mathbf{M} + \mathbf{S} = \mathbf{0} \tag{2.17d}$$

It is clear that (2.17) represents a reducible system of equations and that different possible choices exist concerning the variables to retain in the final group of equations to solve numerically [5]. A possibility is to retain w, $\boldsymbol{\theta}$ and $\mathbf{S}$ such that the final system become:

$$\mathbf{L}^T \mathbf{D}^b \boldsymbol{\kappa} + \mathbf{S} = \mathbf{0} \tag{2.18a}$$

$$\mathbf{S} = \mathbf{D}^s \boldsymbol{\gamma} \tag{2.18b}$$

$$\nabla^T \mathbf{S} + q = 0 \tag{2.18c}$$

From (2.17) the thin plate case can be obtained as a limiting case. In fact, for $\mathbf{D}^s \to \infty$, in order to have a finite value of the shear stresses $\mathbf{S}$, $\boldsymbol{\gamma}$ must go to zero and (2.17b) and (2.14) become the well known constraint of the thin Kirchhoff plate theory:

$$\boldsymbol{\gamma} = \mathbf{e}\,\boldsymbol{\theta} + \nabla w = \mathbf{0} \tag{2.19}$$

Due to the numerous manipulations that will be performed in the next sections, it is useful to introduce a more compact notation. The displacements, i.e. w, θ_x and θ_y, can be arranged in an unique vector $\mathbf{u}$ given by:

$$\mathbf{u} = \begin{Bmatrix} w \\ \theta_x \\ \theta_y \end{Bmatrix} \tag{2.20}$$

Therefore, the following relations hold:

$$\boldsymbol{\kappa}(\boldsymbol{\theta}) = \mathbf{L}^b \mathbf{u} \tag{2.21a}$$

$$\nabla w + \mathbf{e}\boldsymbol{\theta} = \mathbf{L}^s \mathbf{u} \tag{2.21b}$$

where $\mathbf{L}^b$ and $\mathbf{L}^s$ are appropriate operators and equations (2.17) can be written in terms of $\mathbf{u}$:

$$\mathbf{M} = \mathbf{D}^b \mathbf{L}^b \mathbf{u} \tag{2.22a}$$

$$\mathbf{S} = \mathbf{D}^s \mathbf{L}^s \mathbf{u} \tag{2.22b}$$

$$\nabla^T \mathbf{S} + q = 0 \tag{2.22c}$$

$$\mathbf{L}^T \mathbf{M} + \mathbf{S} = \mathbf{0} \tag{2.22d}$$

3. MIXED VARIATIONAL APPROACH TO THE THICK PLATE THEORY

Approaching the thick plate problem by a mixed variational principle is worthwhile since it allows one to consider several reductions and therefore to develop different solution alternatives.

The starting functional is based on the minimum potential energy principle for the bending energy and on the Hu-Washizu principle for the transverse shear energy. Accordingly,

$$\Pi_1(w,\theta,\gamma,\mathbf{S}) = \tfrac{1}{2}\int_A \kappa^T(\theta)\mathbf{D}^b\kappa(\theta)\,dA + \tfrac{1}{2}\int_A \gamma^T\mathbf{D}^s\gamma\,dA$$
$$-\int_A \mathbf{S}^T(\gamma - \nabla w - \mathbf{e}\theta)\,dA - \int_A w\,q\,dA + \Pi_{ext} \tag{3.1}$$

where q is the distributed transverse load and Π_{ext} describes the effects of boundary and other loads.

The problem can be easily split into two parts. Taking the variation of Π_1 with respect to $\mathbf{S}$, we get:

$$\int_A \delta\mathbf{S}^T(\gamma - \nabla w - \mathbf{e}\theta)\,dA = 0 \tag{3.2}$$

which can be interpreted as a constraint on the functional Π_2:

$$\Pi_2(w,\theta,\gamma) = \tfrac{1}{2}\int_A \kappa^T(\theta)\mathbf{D}^b\kappa(\theta)\,dA + \tfrac{1}{2}\int_A \gamma^T\mathbf{D}^s\gamma\,dA$$
$$-\int_A w\,q\,dA + \Pi_{ext} \tag{3.3}$$

If (3.2) is used to express γ in terms of w and θ, a Π_3 functional can be generated from (3.3) as:

$$\Pi_3(w,\theta) = \tfrac{1}{2}\int_A \kappa^T(\theta)\mathbf{D}^b\kappa(\theta)\,dA + \tfrac{1}{2}\int_A \gamma^T(w,\theta)\mathbf{D}^s\gamma(w,\theta)\,dA$$
$$-\int_A w\,q\,dA + \Pi_{ext} \tag{3.4}$$

where γ is no longer an independent variable.

If the constraint (3.2) is imposed in a *strong* (point-wise) sense in going from Π_2 to Π_3, we arrive at the minimum potential energy principle (classical displacement formulation) given by:

$$\Pi(w,\theta) = \tfrac{1}{2}\int_A \kappa(\theta)^T\mathbf{D}^b\kappa(\theta)\,dA + \tfrac{1}{2}\int_A (\nabla w + \mathbf{e}\theta)^T\mathbf{D}^s(\nabla w + \mathbf{e}\theta)\,dA$$

$$- \int_A w\, q\, dA + \Pi_{ext} \tag{3.5}$$

However, as we shall demonstrate in the next section, the problem remains mixed if the constraint is imposed in a *weak* sense .

It is also interesting to note that the limiting case of thin plates (i.e. $\mathbf{D}^s \to \infty$ and $\boldsymbol{\gamma} \to \mathbf{0}$) can be considered starting directly from Π_1 which becomes:

$$\Pi_4(w, \boldsymbol{\theta}, \mathbf{S}) = \tfrac{1}{2} \int_A \boldsymbol{\kappa}^T(\boldsymbol{\theta})\, \mathbf{D}^b\, \boldsymbol{\kappa}(\boldsymbol{\theta})\, dA + \tfrac{1}{2} \int_A \mathbf{S}^T (\nabla w + \mathbf{e}\,\boldsymbol{\theta})\, dA$$

$$- \int_A w\, q\, dA + \Pi_{ext} \tag{3.6}$$

As a last point, note that using the notation introduced at the end of Chapter 2, Π can be rewritten in the more compact form:

$$\Pi(w, \theta) = \tfrac{1}{2} \int_A \mathbf{u}^T \left[\mathbf{L}^{b^T}\, \mathbf{D}^b\, \mathbf{L}^b + \mathbf{L}^{s^T}\, \mathbf{D}^s\, \mathbf{L}^s \right] \mathbf{u}\, dA - \int_A w\, q\, dA + \Pi_{ext} \tag{3.7}$$

4. MIXED FINITE ELEMENT SOLUTION

In the previous sections the equations governing a thick plate problem together with equivalent variational formulations have been presented. In this section a general finite element solution strategy is considered.

Starting from functional Π_1, or an equivalent one, the goals of the finite element approximation are to:

- Construct appropriate finite element discretizations for each of the variables appearing in the functional Π_1, and
- Manipulate the resulting discrete equations in order to reduce the dimension of the global problem to be solved numerically.

Since at the beginning all the variables are retained, the approach is called *mixed*. Therefore, the fields w, θ, γ and $\mathbf{S}$ are independent and different approximation schemes may be used for each of them. Accordingly, we take:

$$w = \mathbf{N}_w \hat{\mathbf{w}} + \mathbf{N}_{w\theta} \hat{\theta} \tag{4.1a}$$

$$\theta = \mathbf{N}_\theta \hat{\theta} \tag{4.1b}$$

$$\gamma = \mathbf{N}_\gamma \hat{\gamma} \tag{4.1c}$$

$$\mathbf{S} = \mathbf{N}_s \hat{\mathbf{S}} \tag{4.1d}$$

where

$$\hat{\mathbf{w}} \ , \ \hat{\theta} \ , \ \hat{\gamma} \ , \ \hat{\mathbf{S}} \tag{4.2a}$$

are the degrees of freedom of the discretized system and

$$\mathbf{N}_w \ , \ \mathbf{N}_{w\theta} \ , \ \mathbf{N}_\gamma \ , \ \mathbf{N}_\theta \ , \ \mathbf{N}_s \tag{4.2b}$$

are the corresponding shape functions. It is noted that the rotational field has been used in order to improve the displacement field approximation and this is explicitly stated by the $\mathbf{N}_{w\theta}$ shape functions.

The variational theorems in the previous section require w and θ to be continuous (C^0) while γ and S may be approximated by piece-wise continuous functions (H^{-1}). Hence interpolation for the shear force and the strain can have parameters which are associated with individual elements; in this case it is possible to eliminate the dependence in the shear parameter at the element level, while at least some of those for the displacement fields must be carried to the global level.

Once independent approximations have been assumed for the four unknown fields, the second step , i.e. a reduction in size of the global finite element problem, can be performed for the case where $\hat{\mathbf{S}}$ and $\hat{\gamma}$ are restricted to an individual element. Accordingly, substituting (4.1) into (3.2) we get:

$$\delta\hat{\mathbf{S}}^T \int_A \mathbf{N}_s^T \left(\mathbf{N}_\gamma \hat{\gamma} - \nabla\mathbf{N}_w \hat{\mathbf{w}} - \mathbf{e}\mathbf{N}_\theta \hat{\theta} \right) dA = \tag{4.3}$$

$$= \delta\hat{\mathbf{S}}^T \left[\left(\int_A \mathbf{N}_s^T \mathbf{N}_\gamma dA \right) \hat{\gamma} - \left(\int_A \mathbf{N}_s^T \nabla\mathbf{N}_w dA \right) \hat{\mathbf{w}} - \left(\int_A \mathbf{N}_s^T \mathbf{e}\mathbf{N}_\theta dA \right) \hat{\theta} \right] = 0$$

Since $\delta\hat{\mathbf{S}}^T$ is arbitrary, the term in the square bracket must vanish and so:

$$\left(\int_A \mathbf{N}_s^T \mathbf{N}_\gamma dA \right) \hat{\gamma} = \left(\int_A \mathbf{N}_s^T \nabla\mathbf{N}_w dA \right) \hat{\mathbf{w}} + \left(\int_A \mathbf{N}_s^T \mathbf{e}\mathbf{N}_\theta dA \right) \hat{\theta} \tag{4.4}$$

which may be written in a more compact form as:

$$\mathbf{F}\,\hat{\gamma} = \mathbf{G}\,\hat{\mathbf{w}} + \mathbf{H}\,\hat{\theta} \tag{4.5}$$

where:

$$\mathbf{F} = \int_A \mathbf{N}_s^T \mathbf{N}_\gamma dA \tag{4.6a}$$

$$\mathbf{G} = \int_A \mathbf{N}_s^T \nabla\mathbf{N}_w dA \tag{4.6b}$$

$$\mathbf{H} = \int_A \mathbf{N}_s^T \mathbf{e}\,\mathbf{N}_\theta dA \tag{4.6c}$$

From (4.5) we can express $\hat{\gamma}$ in terms of $\hat{\mathbf{w}}$ and $\hat{\theta}$:

$$\hat{\gamma} = \mathbf{F}^{-1}\mathbf{G}\hat{\mathbf{w}} + \mathbf{F}^{-1}\mathbf{H}\,\hat{\theta} \tag{4.7}$$

Thus, (4.1c) may be written as

$$\gamma = \mathbf{N}_\gamma \hat{\gamma} = \bar{\mathbf{B}}^s \hat{\mathbf{u}} \tag{4.8}$$

where the unknowns $\hat{\mathbf{w}}$ and $\hat{\theta}$ have been arranged into a unique vector $\hat{\mathbf{u}}$, which is similar to (2.20) and (2.21b). In the same way, the change in curvature (2.21a) may be written as:

$$\kappa = \tilde{\mathbf{B}}^b \hat{\theta} = \mathbf{B}^b \hat{\mathbf{u}} \tag{4.9}$$

where in the above $\mathbf{B}^{\tilde{b}}$ merely adds some zero-columns, associated with $\hat{w}$, to form $\mathbf{B}^b$.

Equations (4.8) and (4.9) can now be inserted into (3.4):

$$\Pi_3(\hat{\mathbf{w}}, \hat{\theta}) = \tfrac{1}{2}\hat{\mathbf{u}}^T \left\{ \int_A [\mathbf{B}^{bT} \mathbf{D}^b \mathbf{B}^b + \bar{\mathbf{B}}^{sT} \mathbf{D}^s \bar{\mathbf{B}}^s] dA \right\} \hat{\mathbf{u}}$$

$$- \int_A w\, q\, dA + \Pi_{ext} \tag{4.10}$$

which represents the mixed finite element version of Π_3.

It is worthwhile to compare (4.10) with the discretized form of Π, which becomes:

$$\Pi(\hat{\mathbf{w}},\hat{\boldsymbol{\theta}}) = \tfrac{1}{2}\hat{\mathbf{u}}^T\left\{\int_A [\mathbf{B}^{b^T}\mathbf{D}^b\mathbf{B}^b + \mathbf{B}^{s^T}\mathbf{D}^s\mathbf{B}^s]\,dA\right\}\hat{\mathbf{u}}$$
$$- \int_A w\,q\,dA + \Pi_{ext} \tag{4.11}$$

where $\mathbf{B}^s$ is the standard displacement representation for the shear strain-displacement equations.

Equations (4.10) and (4.11) are very similar formally but differ since in the first one the the matrix $\bar{\mathbf{B}}^s$ obtained from the mixed approach is present, while in the second one the $\mathbf{B}^s$ is present, which is obtained from the more traditional displacement approach. It has to be noted that in constructing Π_3 no hypotheses are stated about the relations between the unknown fields and from this point of view the constraint equation (3.2) can be satisfied also in a *weak* sense and, therefore, from a finite element point of view, in a more general sense. Instead, in constructing Π, equation (3.2) is imposed in a *strong* (point-wise) sense. This is the main difference between the displacement and the mixed finite element approach.

The choice of the interpolating functions used to approximate each field variable is the most vital and important step of any finite element procedure. Starting from (4.1) different families of plate elements can be generated by making different choices for the interpolating functions. Considerable effort has been devoted to generating shape functions for the displacement fields (transverse displacement and rotations), mostly based on some form of isoparametric interpolation. However, these are often combined with quite poor interpolating functions for the shear strain and stress fields. As an example, collocation functions have been used for the shear field interpolation in some well-performing plate elements, known as Discrete Reissner-Mindlin (DRM) elements [29,30]. The reason for using the collocation functions was justified by the necessity to not over-constraining the shearing strain part of the functional, since in this way (3.2) is satisfied only at a discrete set of points. As it will be shown here, there is no particular reason for choosing such simple shape functions. In fact in the following sections smoother interpolating functions will be adopted for the shear strain and stress fields also.

5. REQUIREMENTS FOR STABILITY AND CONVERGENCE OF A MIXED FINITE ELEMENT SOLUTION

The mathematical conditions that a mixed finite element formulation has to satisfy in order to ensure the stability and the convergence of the solution are embedded in the Babuska-Brezzi conditions [21-23]. These conditions employ specific mathematical arguments and must be checked for each proposed finite element. A thorough evaluation involves considerable calculation, consequently, alternatives which utilize direct computer solutions have been sought.

In the late 1980's, the *mixed patch test* was introduced and shown to generate many of the results needed in the Babuska-Brezzi condition evaluation [24-30]. The mixed patch test is easier and more intuitive to perform and provides necessary and sufficient conditions for the stability and convergence of a mixed finite element. Consequently, in the following discussion we present general results from the mixed patch test for the thick plate formulation discussed above. In Section 6 we propose a set of triangular elements which have external (global) vertex displacement degrees-of-freedom only together with suitable internal unknowns involving displacements, shear strains, and shear forces. In Section 7 we employ results from the mixed patch test to evaluate general characteristics of the proposed elements for applications to thick and thin plate problems. Subsequently, we test the performance of the elements on a set of standard test problems.

FIRST TEST: This part of the mixed patch test consists in checking some simple algebraic inequalities involving the number of unknowns in each variable set. The algebraic requirements for a thick plate formulation are:

$$n_\gamma \geq n_s \qquad n_\theta + n_w \geq n_s \qquad n_s \geq n_w \tag{5.1}$$

where n_w, n_θ, n_γ and n_s stand for the number of degrees-of-freedom in the discretized system for w, $\boldsymbol{\theta}$, $\boldsymbol{\gamma}$ and $\mathbf{S}$ respectively. Equation (5.1) must be satisfied for any generic finite element mesh.

In the following we summarize the steps needed to obtain the above results. Starting from functional (3.1), taking variations with respect to all the variables and arranging the equations in a matrix form leads to:

$$\begin{bmatrix} \mathbf{A} & \mathbf{0} & \mathbf{H}^T & \mathbf{0} \\ \mathbf{0} & \mathbf{0} & \mathbf{G}^T & \mathbf{0} \\ \mathbf{H} & \mathbf{G} & \mathbf{0} & -\mathbf{F} \\ \mathbf{0} & \mathbf{0} & -\mathbf{F}^T & \mathbf{P} \end{bmatrix} \begin{Bmatrix} \hat{\boldsymbol{\theta}} \\ \hat{\mathbf{w}} \\ \hat{\mathbf{S}} \\ \hat{\boldsymbol{\gamma}} \end{Bmatrix} = \begin{Bmatrix} \mathbf{f}_1 \\ \mathbf{f}_2 \\ \mathbf{f}_3 \\ \mathbf{f}_4 \end{Bmatrix} \tag{5.2}$$

where

$$\mathbf{A} = \int_A \tilde{\mathbf{B}}^{b^T} \mathbf{D}^b \tilde{\mathbf{B}}^b \, dA \;, \quad \mathbf{H} = \int_A \mathbf{N}_s^T \mathbf{e} \mathbf{N}_\theta \, dA \tag{5.3a}$$

$$\mathbf{G} = \int_A \mathbf{N}_s^T \nabla \mathbf{N}_w dA \quad , \quad \mathbf{F} = \int_A \mathbf{N}_s^T \mathbf{N}_\gamma dA \tag{5.3b}$$

$$\mathbf{P} = \int_A \mathbf{N}_\gamma^T \mathbf{D}^s \mathbf{N}_\gamma dA \tag{5.3c}$$

and $\mathbf{f}_1$, $\mathbf{f}_2$, $\mathbf{f}_3$ and $\mathbf{f}_4$ account for generalized loading conditions which may include both essential and natural boundary conditions.

Equation (5.2_1) is the weak form of the angular momentum equations, (5.2_2) is the weak form of the transverse linear momentum equation, (5.2_3) is the weak form of the transverse shearing strain-displacement relations and (5.2_4) is the weak form of the transverse shear constitutive equation. We also recall that locking is associated with the transverse shearing behavior as a plate becomes thin.

It was noted in Sections 2 and 3 that mixed formulations for plates are reducible. Similarly, the weak form of a mixed formulation is reducible and there are different ways to perform a reduction on (5.2). As an example, $\hat{\gamma}$ can be condensed: using (5.2_4) $\hat{\gamma}$ can be expressed in terms of $\hat{\mathbf{S}}$ and the result can be substitute in the remaining equations of (5.2). In order to perform this step, the matrix $\mathbf{P}^{-1}\mathbf{F}^T$ must be computed and the following inequality must hold:

$$n_\gamma \geq n_s \tag{5.4}$$

which is the first requirement contained in (5.1). Equation (5.4) implies that the rank of $\mathbf{P}^{-1}$ is not less than the rank of $\mathbf{F}$, and, consequently, the reduction cannot cause a lowering of the rank of the global system (the non-singularity of the $\mathbf{P}$ matrix will be guaranteed if the basis functions used in the shape functions $\mathbf{N}_\gamma$ are linearly independent).

Performing the condensation described above, the system becomes:

$$\begin{bmatrix} \mathbf{A} & \mathbf{0} & \mathbf{H}^T \\ \mathbf{0} & \mathbf{0} & \mathbf{G}^T \\ \mathbf{H} & \mathbf{G} & \mathbf{E} \end{bmatrix} \begin{Bmatrix} \hat{\boldsymbol{\theta}} \\ \hat{\mathbf{w}} \\ \hat{\mathbf{S}} \end{Bmatrix} = \begin{Bmatrix} \mathbf{f}_1' \\ \mathbf{f}_2' \\ \mathbf{f}_3' \end{Bmatrix} \tag{5.5}$$

where

$$\mathbf{E} = -\mathbf{F}\mathbf{P}^{-1}\mathbf{F}^T \tag{5.6}$$

and the loads $\mathbf{f}_i'$ include modifications from the reduction.

The form given in (5.5) is appropriate for evaluating performance at the thin plate limit. Noting from Section 3 that the thin plate limit is equivalent to $\mathbf{D}^s \to \infty$ leads to the result that $\mathbf{E} \to \mathbf{0}$ for this case. Consequently, for a mixed formulation to produce viable results in thin plate applications, the set of equations

$$\begin{bmatrix} \mathbf{A} & \mathbf{0} & \mathbf{H}^T \\ \mathbf{0} & \mathbf{0} & \mathbf{G}^T \\ \mathbf{H} & \mathbf{G} & \mathbf{0} \end{bmatrix} \begin{Bmatrix} \hat{\boldsymbol{\theta}} \\ \hat{\mathbf{w}} \\ \hat{\mathbf{S}} \end{Bmatrix} = \begin{Bmatrix} \mathbf{f}_1' \\ \mathbf{f}_2' \\ \mathbf{f}_3' \end{Bmatrix} \tag{5.7}$$

must have a stable solution. It may be noted that (5.7) follows directly from a discretization of (3.6). This case has been evaluated in references 24 to 27, and satisfaction leads to the second and third part of (5.1).

It is important to emphasize that the conditions in (5.1) represent only a necessary condition for the stability of the solution; however, checking the conditions for different *patches* (including both single elements and meshes with several elements which have a maximum or a minimum number of essential boundary conditions), the requirement becomes very stringent and therefore can be considered also as a sufficient condition for assessing stability, provided that the second test described below is satisfied. In the cited literature (5.1) is usually checked on three standard patches, called respectively *restrained*, *relaxed* and *infinite* patch (e.g. see [4]).

SECOND TEST: The eigenvalues of the stiffness matrix of a patch are computed and the presence of zero eigenvalues in excess of the number of rigid body modes indicates *rank-deficiency* (or zero energy modes). This part of the test is commonly performed on a very small patch of elements (often on a single element) and preferably no boundary conditions are imposed (or if required by the software available only a minimum number are set in order to restrain rigid body motions).

The importance of this second test is related to the fact that solving more general problems using rank-deficient elements can lead to instability in the solution and often results in non converging solutions (such as oscillations fluctuating around the exact solution) or it can occasionally result in a singular global stiffness matrix. On the other hand, it can also happen that the boundary conditions used result in a non-singular coefficient matrix, such that no zero-energy modes are globally present. It is clear that these uncertainties are such that the presence of excess zero eigenvalues at a multi element level must be considered as an index of possible ill-conditioned behavior and of non-robustness of the associated discretized problem. If such singularity exists only for a single element the issue is not so clear but remain undesiderable.

An additional aspect which may be recovered from the eigen-analysis is the full evaluation of the number of modes available in an element to represent the bending and the shear response. The eigenvalues of the bending modes are proportional to thickness to the third power, whereas, those for shear are proportional to the thickness. By performing the eigen-analysis for a wide range of thicknesses (we normally scale the modulus so that the bending stiffness remains constant), the number of modes for bending and shear

may be determined. In Section 7.3 we discuss this aspect in more detail for the elements evaluated in this study.

THIRD TEST: This part of the patch test assesses consistency of results. In the plate problem we need to ensure that constant curvature states are exactly recovered. Since the element is formulated in cartesian coordinates the metric is independent of units and thus this strong satisfaction is needed [4]. Moreover, states for constant transverse shear in the absence of bending effects must also be included (since other cases would require a linear varying curvature field).

The third test is merely the classical patch requirement originally proposed by Bazeley *et al.* in their classical paper [7].

6. PROPOSED FINITE ELEMENTS FOR THE THICK PLATE PROBLEM

As pointed out in the introduction, some of the purposes of the present paper are to:

- show that smooth interpolating function can be used for the shear strain and stress fields as well as for the displacement fields,
- discuss an existing element and introduce some new simple triangular elements,
- illustrate the performance of these elements on some standard test problems.

The first two purposes are presented in this section, the last one in the next section.

6.1 General features and degrees-of-freedom

The finite elements described here are all based on the mixed approach to the plate problem discussed previously.

The elements are triangular and the shape functions are expressed in terms of area coordinates, L_i with $i=1,2,3$ [4]. Thus, the region occupied by each element may be expressed as

$$\mathbf{x} = L_i \hat{\mathbf{x}}_i \tag{6.1}$$

where $0 \le L_i \le 1$, $L_1+L_2+L_3=1$, $\mathbf{x}=\{x, y\}^T$ and $\hat{\mathbf{x}}_i=\{\hat{x_i}, \hat{y_i}\}^T$ with $i=1,2,3$ are the nodal coordinates.

Each element has three external (global) displacement degrees-of-freedom at each vertex of the triangle: the transverse displacement $\hat{w}_i$ and the two rotations $\hat{\theta}_{ix}$ and $\hat{\theta}_{iy}$. In addition, to correct some deficiency in meeting mixed patch test requirements or to increase overall order of interpolation, the elements have been provided with internal degrees-of-freedom for the displacements. Internal degrees-of-freedom are preferred to external ones since they can be easily eliminated (by static condensation) at the element level.

In addition to differences in the internal degree-of-freedom structure, the elements considered below also differ in the interpolating functions adopted for shear strain and forces. In general, as simple interpolation functions as possible are introduced for the part of the problem governing the bending behavior, while special attention is devoted to the shear contribution since it is the source of locking effects.

6.2 Element EL1

In addition to the three vertex degrees-of-freedom, this element has two internal rotational degrees-of-freedom associated with a cubic bubble function, for a total of eleven displacement degrees-of-freedom. For the rotational

field, the interpolation is linear plus the bubble function and in terms of area coordinates it is written as:

$$\theta = \sum_{i=1}^{3} L_i \hat{\theta}_i + 27 L_1 L_2 L_3 \Delta\hat{\theta} \tag{6.2}$$

where

$$\hat{\theta}_i = \begin{Bmatrix} \hat{\theta}_{ix} \\ \hat{\theta}_{iy} \end{Bmatrix}, \qquad \Delta\hat{\theta} = \begin{Bmatrix} \Delta\hat{\theta}_x \\ \Delta\hat{\theta}_x \end{Bmatrix} \tag{6.3}$$

The transverse displacement interpolation is taken as a simple linear function, enhanced by quadratic terms expressed in terms of the normal components of the nodal rotations for each side of the element. Accordingly,

$$w = \sum_{i=1}^{3} L_i \hat{w}_i - \sum_{i=1}^{3} L_i L_j \frac{\theta_{jn} - \theta_{in}}{2 l_k} \tag{6.4}$$

where the indices i, j, k are a cyclic permutation which may be written compactly as: $j = mod(i,3)+1$ and $k = mod(j,3)+1$ [(1)]. In the following whenever an index i, j, or k is referred to a side of an element instead of a node, it indicates the side opposite to a vertex. Therefore, in (6.4) with l_k we denote the length of the k-side, i.e. the length of the side between the i and j nodes and opposite to the k node.

The shear strain and the shear stress are assumed constant over each element, i.e. unit interpolating functions for $\mathbf{N}_\gamma$ and $\mathbf{N}_s$ are adopted:

$$\gamma = \mathbf{N}_\gamma \hat{\gamma} = \hat{\gamma} = \bar{\gamma} = \begin{Bmatrix} \bar{\gamma}_x \\ \bar{\gamma}_y \end{Bmatrix} \tag{6.5}$$

$$\mathbf{S} = \mathbf{N}_s \hat{\mathbf{S}} = \hat{\mathbf{S}} = \bar{\mathbf{S}} = \begin{Bmatrix} \bar{S}_x \\ \bar{S}_y \end{Bmatrix} \tag{6.6}$$

where a bar in (6.5) and (6.6) represents the fact that they are constant over the element. This element was originally introduced and partially analyzed in [31].

6.3 Element EL2

This element has the usual three vertex displacement degrees-of-freedom plus six internal rotational degrees-of-freedom, where we associate two with each k-side and denote them as $\Delta\hat{\theta}_x^k$ and $\Delta\hat{\theta}_y^k$. Therefore the element has a total of fifteen displacement degrees-of-freedom. The choice of the internal

(1) The *mod(i,j)* is a standard programming remainder function equal to *i-(i/j)*j* where integer arithmetic is used to compute *i/j*.

degrees-of-freedom is the main difference between this element and the previous one, difference which is also reflected in the choice of the interpolating functions.

For the transverse displacement the same shape functions as for EL1 have been selected, i.e.:

$$w = \sum_{i=1}^{3} L_i \hat{w}_i - \sum_{i=1}^{3} L_i L_j \frac{\theta_{jn} - \theta_{in}}{2\, l_k} \tag{6.7}$$

while the rotational fields are now approximated by:

$$\theta = \sum_{i=1}^{3} L_i \hat{\theta}_i + \sum_{i=1}^{3} L_i^2 L_j L_k \beta_k \Delta\hat{\theta}_k \tag{6.8}$$

where:

$$\Delta\hat{\theta}_k = \begin{Bmatrix} \Delta\hat{\theta}_x^k \\ \Delta\hat{\theta}_y^k \end{Bmatrix} \tag{6.9}$$

Note that:

- the modification of the θ field is made by fourth order polynomials of type $L_i^2 L_j L_k$, that are zero along all boundaries of the element and thus maintains compatibility *a priori*;
- different choices have been selected for the β_k matrix in (6.8) and these are classified as follow:

$$\textit{version A} \qquad \beta_k = \mathbf{n}_k \mathbf{1}^T = \begin{Bmatrix} n_x^k \\ n_y^k \end{Bmatrix} [1 \quad 1] \tag{6.10a}$$

$$\textit{version B} \qquad \beta_k = \mathbf{t}_k \mathbf{1}^T = \begin{Bmatrix} t_x^k \\ t_y^k \end{Bmatrix} [1 \quad 1] \tag{6.10b}$$

$$\textit{version C} \qquad \beta_k = \mathbf{1}\,\mathbf{1}^T = \begin{bmatrix} 1 & 0 \\ 0 & 1 \end{bmatrix} = \mathbf{I} \tag{6.10c}$$

where $\mathbf{n}_k$ and $\mathbf{t}_k$ are respectively the outward normal and the tangential vector along the k-side.

Due to the particular expression for β_k, in version A and B the sum of the internal degrees-of-freedom along each side is used and therefore it is possible to introduce it directly as the only unknown, say $\Delta\hat{\theta}_k^m$, such that these elements have only twelve displacement degrees-of-freedom. Therefore, as a result of (6.10a) and (6.10b), $\Delta\hat{\theta}_k^m$ can be interpreted as a hierarchical rotation associated with the k-side, respectively normal to it in version A and tangential in version B. Version C is instead a truly fifteen degree-of-freedom element and there is no clear physical meaning for the internal unknowns.

The strain shear field is interpolated linearly:

$$\gamma = \sum_{i=1}^{3} L_i \hat{\gamma}_i \tag{6.11a}$$

while in the previous element it is assumed constant. The $\hat{\gamma}_i$ parameters are associated with the nodes of the element; however, these parameters may also be expressed in terms of local components of the shear along the perimeter of the element (two on each side). It is then possible to *constrain* the tangential shear to be constant along each side, therefore reducing the number of independent shear parameters to three [29,30]. The reason for this type of constraint is the necessity to satisfy the algebraic inequalities on the number of degrees-of-freedom required by the mixed patch test. This constraint is expressed by:

$$\hat{\gamma}_i = \frac{1}{\Delta_i} \begin{bmatrix} n_y^j & -n_y^k \\ -n_x^j & n_x^k \end{bmatrix} \begin{Bmatrix} \bar{\gamma}_k \\ \bar{\gamma}_j \end{Bmatrix} \tag{6.11b}$$

where $\Delta_i = n_x^k n_y^j - n_y^k n_x^j$ and $\hat{\gamma}_j$, $\hat{\gamma}_k$ are the constant shear strain along the j and the k side.

The shear stress field is still assumed constant:

$$\mathbf{S} = \mathbf{N}_s \hat{\mathbf{S}} = \hat{\mathbf{S}} = \bar{\mathbf{S}} = \begin{Bmatrix} \bar{S}_x \\ \bar{S}_y \end{Bmatrix} \tag{6.12}$$

The use of interpolations (6.11a) or (6.11b) and (6.12) satisfies the mixed patch test requirements given in Section 5. In the numerical experiments reported below we use (6.11b).

6.5 Element EL3

This element has the same internal degrees-of-freedom as EL2. It also has the same interpolating functions for the displacements:

$$w = \sum_{i=1}^{3} L_i \hat{w}_i - \sum_{i=1}^{3} L_i L_j \frac{\theta_{jn} - \theta_{in}}{2 l_k} \tag{6.13}$$

$$\theta = \sum_{i=1}^{3} L_i \hat{\theta}_i + \sum_{i=1}^{3} L_i^2 L_j L_k \beta_k \Delta\hat{\theta}_k \tag{6.14}$$

and for the shear strain field:

$$\gamma = \sum_{i=1}^{3} L_i \hat{\gamma}_i \tag{6.15}$$

where $\hat{\gamma}_i$ is again computed from (6.11b). The shear stress field is modified to a form identical to that of the shear strain and a linear interpolation has been chosen:

$$\mathbf{S} = \sum_{i=1}^{3} L_i \hat{\mathbf{S}}_i \tag{6.16}$$

where the parameters $\hat{\mathbf{S}}_i$ are computed from (6.11b) with γ replace by S. Also for this element the versions A, B and C described in the previous sub-section have been considered.

6.6 Stiffness matrix and load vector

The procedure for the construction of the stiffness matrix has been split into two steps, the reason of which is clear by looking at (3.7) and (4.10). In the first step the part due to the bending, $\mathbf{K}^b$, is computed while in the second one the part due to the shear, $\mathbf{K}^s$,is computed. The two matrices are summed in order to obtain the total stiffness matrix:

$$\mathbf{K} = \mathbf{K}^b + \mathbf{K}^s \tag{6.17}$$

From (4.10) we get that:

$$\mathbf{K}^b = \int_A (\mathbf{L}\mathbf{N}_\theta)^T \mathbf{D}^b (\mathbf{L}\mathbf{N}_\theta) dA \tag{6.18}$$

$$\mathbf{K}^s = \int_A \bar{\mathbf{B}}^{s^T} \mathbf{D}^s \bar{\mathbf{B}}^s dA \tag{6.19}$$

where a general approach for the construction of $\bar{\mathbf{B}}^s$ is given in Section 4.

It is noted that, due to particular choices for the shape functions, simplifications can occur. For example, in EL1, the shape functions for the shear strain and stress fields are constant in each element, hence, the $\bar{\mathbf{B}}^s$ matrix is also constant and may be computed directly in terms of the displacement parameters. It is noted that evaluation of $\mathbf{F}$ and $\mathbf{G}$ in (4.6a,b) for EL1 and EL2 may be performed using 1-point quadrature; however, exact evaluation of (4.6c) requires more than 3-points (e.g., either a 4-point or 7-point formula as described in [4]). Inexact integration (i.e., reduced quadrature) may also be used, and the results in [31] are equivalent to EL1 based on a 1-point quadrature for this term as well (we call this element EL1R). We note this reduced quadrature is associated only with the specification of the strain displacement equation and thus do not preclude using this element with nonlinear constitutive models. This is in contrast with the use of reduced quadrature in displacements models. In EL3 it is necessary to perform all the steps in equations (4.5)-(4.8) in order to construct $\bar{\mathbf{B}}^s$. Numerical evaluation of the integrals requires multi-point quadrature to obtain correct rank in the results. Except as noted for EL1R, all integrals are computed exactly using a sufficiently high order quadrature.

For the results reported in the next section, the finite element load vector for distributed transverse loads q is computed consistently using the shape functions in the interpolation for the transverse displacement, w.

7.1 NUMERICAL PERFORMANCE

Several tests have been performed in order to evaluate the numerical performance of the elements discussed in the previous section. The elements have been implemented into the Finite Element Analysis Program (FEAP) and this environment has been used for all the computations [4,5].

For the cases where no analytical or series solution of a problem is available, the numerical solution has been compared with those obtained using the DRM3 element [30]. This is a triangular element endowed with an external rotational degree-of-freedom for each edge; it uses quadratic interpolating functions for the rotations, cubic for the transverse displacement, linear for the transverse shear strain and Dirac delta functions for the tangential component of the transverse shear stress at the center of each edge.

The test problems are organized in the following order:

- First patch test: Algebraic constraint count requirement
- Second patch test: Eigenvalue evaluation for rank and locking
- Third patch test: Consistency tests for pure bending, pure twist, pure shear
- Square plate with simply supported and clamped boundaries
- Circular plate with simply supported and clamped boundaries
- Skew cantilever plate
- Simply supported skew plate

Only uniform loading is considered since it is well known that the transverse displacement for a concentrated load is infinite for a theory which includes the effects of shear deformation.

7.1 First patch test: Algebraic constraint count requirement

For all the elements discussed in the previous section the algebraic requirements in (5.1) have been checked for single elements with all boundaries fixed and also with a minimum number restrained to prevent rigid body modes. In addition, the counts have been constructed for regular square meshes (of the type shown below for the square plates). For the cases in which $\mathbf{S}$ is a constant in each element, the count condition reduces to the evaluation of n_s compared to n_w for all meshes. The other conditions are always satisfied since by construction (5.1_1) has n_γ greater or equal to n_s and the θ has two internal bubble modes which exactly balances n_s, thus satisfying (5.1_2). For the case where $\mathbf{S}$ is linear in each element it is necessary to check both (5.1_2) and (5.1_3).

For the types of meshes considered, all the elements described in this work pass the first patch test.

7.2 Second patch test: Eigenvalue evaluation for rank and locking

The first part of the second patch test consists in checking that the stiffness matrix of a single element has no zero eigenvalues in excess of the number of rigid body modes, as described in Section 5.

The second part is based on a set of problems which approach the limiting case of a thin plate. For a one-element mesh the ratio between thickness, t, and side length, L, is varied between the values 10 and 1E-5; Young's modulus is also varied in order to maintain a constant value of the bending stiffness D. In this way, the modes in the element associated with bending effects remain approximately constant, while those influenced by shear increase by L/t squared. This test is very useful to check the tendency of an element to lock. It also indicates whether all modes included in each interpolation are available in the actual solution process. Finally, this part of the test can assess whether any of the eigenvalues tends to zero in the limiting case of thin plates.

Both EL1 and EL2 (and EL1R) do not pass the first part of this patch test since they show an extra zero-energy mode. Conversely, EL3 passes the first part. All the elements behave properly in the second part of this test. We noted that in repeating the above process using a 2-element mesh all aspects of the eigen-analysis are satisfied.

7.3 Third patch test: Consistency test for pure bending, pure twist and pure shear

The third patch test was conducted on a square plate of arbitrary triangles as in [30] and the following boundary conditions in terms of load and displacement have been considered:

- pure bending - distributed constant edge moment along one edge, the opposite edge is clamped and all lateral boundary tangential rotations are fixed;
- pure twist - distributed constant edge twisting moments along all four sides, three corner nodes are restrained to prevent rigid body motion.
- pure shear - distributed constant edge forces on one edge, the opposite edge is clamped, and all rotations fixed in order to prevent bending;

All elements pass the third patch test.

7.4 Square plate with simply supported and clamped boundaries

A square plate is modeled using meshes that differ in the orientation of the elements (the two mesh types are labeled A and B in Fig. 7.1). Three boundary conditions are considered: *soft* simply supported, *hard* simply

supported and clamped. For the soft simply supported boundary condition only nodal w are restrained.[1] A discussion of the soft and hard simply supported boundary condition is given in [2,5].

The material properties of the plate are:

$$E = 10.92 \ , \quad \nu = 0.3$$

the side length is $L = 10$, the uniform load $q = 1.0$ and the thickness $t = 0.1$. Since $t/L = 0.01$ the plate is quite thin and the analytical solutions from thin plate theory are reported. In order to check the tendency to lock, also a clamped square plate of thickness $t = 0.01$ is considered ($t/L = 0.001$). For comparison purposes to indicate the importance of shear deformation, a second solution obtained from the thick plate theory is reported whenever it was computed.

Mesh	EL1R	EL1	EL2-A	EL2-B	EL2-C	EL3-A	EL3-B	EL3-C
2x2	4.25559	3.80303	3.78490	3.73507	3.82509	3.44894	3.57813	3.65168
4x4	4.16761	4.01023	4.00549	3.99577	4.01650	3.75596	3.88395	3.92582
8x8	4.11947	4.06053	4.05904	4.05638	4.06262	4.01332	4.02984	4.06683
16x16	4.09766	4.07375	4.07316	4.07215	4.07458	4.06828	4.06823	4.07059
ser.sol.	4.06235	4.06235	4.06235	4.06235	4.06235	4.06235	4.06235	4.06235

Table 7.1: Simply supported square plate $t/L = 0.01$ - soft boundary, mesh A - : displacement at the center ($\times 10^{-4}$)

Mesh	EL1R	EL1	EL2-A	EL2-B	EL2-C	EL3-A	EL3-B	EL3-C
2x2	4.36249	3.89112	3.87954	3.86496	3.90801	1.84893	2.96230	3.28394
4x4	4.18201	4.02767	4.02407	4.01834	4.03291	3.39095	3.76413	3.86085
8x8	4.12165	4.07434	4.06218	4.05984	4.06561	3.98758	4.01635	4.03095
16x16	4.09797	4.06742	4.07376	4.07280	4.07517	4.06712	4.06742	4.06989
ser.sol.	4.06235	4.06235	4.06235	4.06235	4.06235	4.06235	4.06235	4.06235

Table 7.2: Simply supported square plate $t/L = 0.01$ - soft boundary, mesh B - : displacement at the center ($\times 10^{-4}$)

Mesh	EL1R	EL1	EL2-A	EL2-B	EL2-C	EL3-A	EL3-B	EL3-C
2x2	4.13885	3.78197	3.76580	3.71603	3.80036	3.40554	3.55409	3.61583
4x4	4.08829	3.99457	3.99086	3.98073	3.99893	3.74116	3.87180	3.90786
8x8	4.07080	4.04930	4.04868	4.04729	4.05011	4.00436	4.02170	4.02831
16x16	4.06607	4.06098	4.06086	4.06065	4.06116	4.05731	4.05785	4.05823
ser.thin	4.06235	4.06235	4.06235	4.06235	4.06235	4.06235	4.06235	4.06235
ser.thick	4.06446	4.06446	4.06446	4.06446	4.06446	4.06446	4.06446	4.06446

Table 7.3: Simply supported square plate $t/L = 0.01$ - hard boundary, mesh A - : displacement at the center ($\times 10^{-4}$)

---

(1) We note that the presence of $\hat{\boldsymbol{\theta}}$ in the interpolation for $\mathcal{W}$, (4.1a), will produce non-zero boundary displacements. A work is in progress to evaluate the implications of this error.

Mesh	EL1R	EL1	EL2-A	EL2-B	EL2-C	EL3-A	EL3-B	EL3-C
2x2	4.07687	3.53107	3.50953	3.41852	3.55041	1.63264	2.74932	2.96013
4x4	4.06692	3.95148	3.94779	3.93387	3.95505	3.31893	3.70239	3.77628
8x8	4.06513	4.03897	4.03831	4.03595	4.03963	3.96521	3.99532	4.00435
16x16	4.06464	4.05839	4.05825	4.05778	4.05854	4.05289	4.05366	4.05416
ser.thin	4.06235	4.06235	4.06235	4.06235	4.06235	4.06235	4.06235	4.06235
ser.thick	4.06446	4.06446	4.06446	4.06446	4.06446	4.06446	4.06446	4.06446

Table 7.4: Simply supported square plate $t/L = 0.01$ - hard boundary, mesh B - : displacement at the center ($\times 10^{-4}$)

Mesh	EL1R	EL1	EL2-A	EL2-B	EL2-C	EL3-A	EL3-B	EL3-C
2x2	1.20690	0.83401	0.81729	0.73867	0.84951	0.32629	0.58247	0.64096
4x4	1.26026	1.14267	1.13795	1.12044	1.14751	0.86492	1.02366	1.05397
8x8	1.26625	1.23808	1.23727	1.23480	1.23900	1.19813	1.21368	1.21889
16x16	1.26748	1.26068	1.26053	1.26010	1.26088	1.25755	1.25785	1.25837
ser.thin	1.260	1.260	1.260	1.260	1.260	1.260	1.260	1.260
ser.thick	1.262	1.262	1.262	1.262	1.262	1.262	1.262	1.262

Table 7.5: Clamped square plate $t/L = 0.01$ - mesh A - : displacement at the center ($\times 10^{-4}$)

Mesh	EL1R	EL1	EL2-A	EL2-B	EL2-C	EL3-A	EL3-B	EL3-C
2x2	1.44839	0.93615	0.91508	0.84510	0.95945	0.37724	0.65819	0.74898
4x4	1.31030	1.18511	1.18043	1.17030	1.19094	0.92596	1.07568	1.11412
8x8	1.27825	1.24991	1.24911	1.24751	1.25095	1.21711	1.22933	1.23589
16x16	1.27046	1.26377	1.26362	1.26327	1.26398	1.26130	1.26141	1.26217
ser.thin	1.260	1.260	1.260	1.260	1.260	1.260	1.260	1.260
ser.thick	1.262	1.262	1.262	1.262	1.262	1.262	1.262	1.262

Table 7.6: Clamped square plate $t/L = 0.01$ - mesh B - : displacement at the center ($\times 10^{-4}$)

Mesh	EL1R	EL1	EL2-A	EL2-B	EL2-C	EL3-A	EL3-B	EL3-C
2x2	1.20509	0.83024	0.81315	0.73205	0.84599	0.27526	0.57110	0.63208
4x4	1.25797	1.13803	1.13282	1.11301	1.14328	0.65730	0.99698	1.03791
8x8	1.26381	1.23452	1.23349	1.23020	1.23565	1.03491	1.18921	1.20485
16x16	1.26500	1.25790	1.25770	1.25709	1.25814	1.20498	1.24607	1.25039
ser.thin	1.260	1.260	1.260	1.260	1.260	1.260	1.260	1.260
ser.thick	1.262	1.262	1.262	1.262	1.262	1.262	1.262	1.262

Table 7.7: Clamped square plate $t/L = 0.001$ - mesh A - : displacement at the center ($\times 10^{-7}$)

Mesh	EL1R	EL1	EL2-A	EL2-B	EL2-C	EL3-A	EL3-B	EL3-C
2x2	1.44588	0.93098	0.90941	0.83780	0.95474	0.32088	0.64443	0.73897
4x4	1.30768	1.18006	1.17488	1.16351	1.18639	0.71867	1.04882	1.09960
8x8	1.27567	1.24616	1.24515	1.24315	1.24745	1.07257	1.20731	1.22419
16x16	1.26792	1.26092	1.26071	1.26030	1.26118	1.21804	1.25109	1.25553
ser.thin	1.260	1.260	1.260	1.260	1.260	1.260	1.260	1.260
ser.thick	1.262	1.262	1.262	1.262	1.262	1.262	1.262	1.262

Table 7.8: Clamped square plate $t/L = 0.001$ - mesh B - : displacement at the center ($\times 10^{-7}$)

7.5 Circular plate with simply supported and clamped boundaries

A circular plate under uniform load is a case in which an analytical solution can be computed in closed form. Both the case of simply supported and clamped boundaries have been considered. The radius R is set equal to 5.0 and two values of the thickness ($t = 0.1$ and $t = 1.0$) have been analyzed, in order to consider a thin plate and a thick plate case. The properties of the material are:

$$E = 10.92 \ , \quad \nu = 0.3$$

and the load is $q = 1.0$ (Fig. 7.2).

Mesh	EL1R	EL1	EL2-A	EL2-B	EL2-C	EL3-A	EL3-B	EL3-C
6	42215.8	39431.8	39370.1	39143.5	39535.5	37026.4	38176.4	38519.5
24	40460.9	39657.6	39640.1	39578.6	39688.8	38432.7	39009.8	39166.5
96	39943.4	39732.6	39727.4	39714.3	39741.0	39411.6	39537.1	39580.9
384	39802.6	39744.3	39742.8	39739.4	39746.5	39707.5	39711.9	39718.3
1536	39764.4	39747.5	39746.9	39746.0	39748.0	39743.1	39742.5	39744.1
ex.sol.	39831.5	39831.5	39831.5	39831.5	39831.5	39831.5	39831.5	39831.5

Table 7.9: Simply supported circular plate - thickness = 0.1 - : displacement at the center

Mesh	EL1R	EL1	EL2-A	EL2-B	EL2-C	EL3-A	EL3-B	EL3-C
6	43.9037	41.1626	41.1024	40.9740	41.2653	40.8041	40.7360	40.9389
24	42.2235	41.4296	41.4131	41.3696	41.4588	41.3589	41.3225	41.3949
96	41.7139	41.5103	41.5060	41.4947	41.5177	41.5014	41.4906	41.5120
384	41.5797	41.5286	41.5276	41.5247	41.5305	41.5273	41.5244	41.5301
1536	41.5459	41.5331	41.5329	41.5322	41.5336	41.5329	41.5321	41.5336
ex.sol.	41.5994	41.5994	41.5994	41.5994	41.5994	41.5994	41.5994	41.5994

Table 7.10: Simply supported circular plate - thickness = 1.0 - : displacement at the center

Mesh	EL1R	EL1	EL2-A	EL2-B	EL2-C	EL3-A	EL3-B	EL3-C
6	9119.24	6049.46	5946.39	5301.04	6135.52	2397.05	4032.29	4614.38
24	9640.34	8774.99	8748.73	8642.32	8802.90	6545.31	7821.20	8082.37
96	9738.15	9523.66	9518.14	9499.78	9531.27	9148.89	9682.22	9357.07
384	9760.75	9708.70	9707.56	9704.22	9710.57	9677.57	9311.25	9686.12
1536	9766.35	9753.53	9753.26	9752.52	9753.99	9751.27	9750.82	9751.85
ex.sol.	9783.48	9783.48	9783.48	9783.48	9783.48	9783.48	9783.48	9783.48

Table 7.11: Clamped circular plate - thickness = 0.1 - : displacement at the center

Mesh	EL1R	EL1	EL2-A	EL2-B	EL2-C	EL3-A	EL3-B	EL3-C
6	10.8377	8.0392	7.9699	7.8099	8.1240	7.5160	7.4412	7.6672
24	11.4059	10.6006	10.5834	10.5359	10.6287	10.5202	10.4805	10.5554
96	11.5066	11.3022	11.2980	11.2864	11.3096	11.2932	11.2820	11.3037
384	11.5285	11.4774	11.4764	11.4735	11.4793	11.4761	11.4732	11.4789
1536	11.5334	11.5207	11.5204	11.5197	11.5211	11.5204	11.5197	11.5211
ex.sol.	11.5513	11.5513	11.5513	11.5513	11.5513	11.5513	11.5513	11.5513

Table 7.12: Clamped circular plate - thickness = 1.0 - : displacement at the center

7.6 Skew cantilever plates

Three skew cantilever plates have been analyzed using different values of the skew angle, β. The 8×8 mesh with $\beta = 40^{\circ}$ is represented in Fig. 7.3. The material properties are:

$$E = 100 \ , \quad \nu = 0.3$$

the thickness is 4.0, the side length 100 and the load 1.0

Since no closed solution is known, the numerical results are compared with those found in [30] (labeled DRM3).

Mesh	EL1R	EL1	EL2-A	EL2-B	EL2-C	EL3-A	EL3-B	EL3-C	DRM3
2x2	1.34410	1.17926	1.17501	1.16114	1.18402	1.10184	1.12820	1.15132	1.3557
4x4	1.39932	1.35210	1.35088	1.34672	1.35361	1.31290	1.32341	1.33383	1.4024
8x8	1.42034	1.40800	1.40772	1.40699	1.40832	1.40185	1.40219	1.40387	1.4204
16x16	1.42727	1.42377	1.42370	1.42353	1.42386	1.42284	1.42273	1.42301	1.4269

Table 7.13: Skew cantilever plate - angle 20° mesh A - : displacement at node 1 ($\times Et^3/qL^4$)

Mesh	EL1R	EL1	EL2-A	EL2-B	EL2-C	EL3-A	EL3-B	EL3-C	DRM3
2x2	1.06379	0.96769	0.96515	0.95999	0.97035	0.96693	0.95842	0.96613	1.0704
4x4	1.04963	1.02099	1.02023	1.01861	1.02187	1.00889	1.01099	1.01543	1.0489
8x8	1.04592	1.03740	1.03717	1.03681	1.03765	1.03455	1.03467	1.03573	1.0440
16x16	1.04463	1.04207	1.04200	1.04192	1.04214	1.04151	1.04146	1.04170	1.0436

Table 7.14: Skew cantilever plate - angle 20° mesh A - : displacement at node 2 ($\times Et^3/qL^4$)

Mesh	EL1R	EL1	EL2-A	EL2-B	EL2-C	EL3-A	EL3-B	EL3-C	DRM3
2x2	1.38237	1.27495	1.26600	1.27996	1.28146	1.18858	1.20579	1.25187	1.5438
4x4	1.39792	1.36850	1.36655	1.36736	1.37012	1.33896	1.34409	1.35763	1.4446
8x8	1.41655	1.40902	1.40881	1.40839	1.40932	1.40537	1.40482	1.40700	1.4285
16x16	1.42447	1.42230	1.42226	1.42210	1.42238	1.42184	1.42164	1.42202	1.4275

Table 7.15: Skew cantilever plate - angle 20° mesh B - : displacement at node 1 ($\times Et^3/qL^4$)

Mesh	EL1R	EL1	EL2-A	EL2-B	EL2-C	EL3-A	EL3-B	EL3-C	DRM3
2x2	1.00047	0.94085	0.94241	0.92947	0.94277	0.95441	0.94060	0.94780	1.0782
4x4	1.02043	1.00367	1.00392	1.00065	1.00421	1.00827	1.00474	1.00656	1.0388
8x8	1.03450	1.02888	1.02884	1.02808	1.02909	1.02884	1.02824	1.02893	1.0386
16x16	1.04041	1.03869	1.03869	1.03849	1.03876	1.03842	1.03825	1.03849	1.0413

Table 7.16: Skew cantilever plate - angle 20° mesh B - : displacement at node 2 ($\times Et^3/qL^4$)

Mesh	EL1R	EL1	EL2-A	EL2-B	EL2-C	EL3-A	EL3-B	EL3-C	DRM3
2x2	1.03872	0.88110	0.87672	0.86517	0.88764	0.77614	0.80836	0.85333	1.0637
4x4	1.11324	1.06333	1.06189	1.05848	1.06542	1.01776	1.02705	1.04477	1.1266
8x8	1.15618	1.14222	1.14191	1.14119	1.14271	1.13417	1.13430	1.13714	1.1619
16x16	1.17613	1.17215	1.17207	1.17188	1.17227	1.17072	1.17058	1.17104	1.1789

Table 7.17: Skew cantilever plate - angle 40° mesh A - . displacement at node 1 ($\times Et^3/qL^4$)

Mesh	EL1R	EL1	EL2-A	EL2-B	EL2-C	EL3-A	EL3-B	EL3-C	DRM3
2x2	.503829	.452927	.451596	.448117	.454940	.427867	.432092	.443428	.5329
4x4	.530757	.516100	.515720	.514750	.516686	.499688	.503182	.508605	.5381
8x8	.541662	.537132	.535705	.536768	.537285	.534328	.534377	.535235	.5426
16x16	.545684	.544102	.544079	.543976	.544149	.543499	.543421	.543607	.5456

Table 7.18: Skew cantilever plate - angle 40° mesh A - : displacement at node 2 ($\times Et^3/qL^4$)

Mesh	EL1R	EL1	EL2-A	EL2-B	EL2-C	EL3-A	EL3-B	EL3-C	DRM3
2x2	0.90890	0.81149	0.79301	0.80416	0.81842	0.63153	0.67846	0.09629	1.2955
4x4	1.02576	0.98925	0.98413	0.98374	0.99163	0.88491	0.90982	0.91707	1.1777
8x8	1.11333	1.10507	1.10434	1.10432	1.10548	1.08240	1.08455	1.08582	1.1646
16x16	1.15622	1.15488	1.15479	1.15474	1.15495	1.15196	1.15197	1.15222	1.1720

Table 7.19: Skew cantilever plate - angle 40° mesh B - : displacement at node 1 ($\times Et^3/qL^4$)

Mesh	EL1R	EL1	EL2-A	EL2-B	EL2-C	EL3-A	EL3-B	EL3-C	DRM3
2x2	.474172	.453228	.452710	.452275	.454026	.455788	.454529	.460198	.6182
4x4	.503837	.500239	.500357	.500049	.500326	.503462	.502432	.503633	.5435
8x8	.527918	.526734	.526774	.526609	.526770	.529236	.528862	.529080	.5375
16x16	.538730	.538197	.538194	.538136	.538218	.538550	.538484	.538563	.5411

Table 7.20: Skew cantilever plate - angle 40° mesh B - : displacement at node 2 ($\times Et^3/qL^4$)

Mesh	EL1R	EL1	EL2-A	EL2-B	EL2-C	EL3-A	EL3-B	EL3-C	DRM3
2x2	.678039	.581632	.578428	.572782	.587447	.527953	.536139	.563838	.7416
4x4	.747229	.707712	.706311	.703916	.710449	.673499	.675213	.688740	.7814
8x8	.802835	.791187	.790819	.790376	.791804	.783209	.782968	.785495	.8192
16x16	.834565	.831366	.831276	.831180	.831522	.829753	.829661	.830095	.8435

Table 7.21: Skew cantilever plate - angle 60° mesh A - : displacement at node 1 ($\times Et^3/qL^4$)

Mesh	EL1R	EL1	EL2-A	EL2-B	EL2-C	EL3-A	EL3-B	EL3-C	DRM3
2x2	.107921	.100257	.099939	.097700	.101116	.086046	.089227	.096504	.1259
4x4	.134221	.130870	.130666	.130585	.131142	.123669	.124438	.127179	.1411
8x8	.146709	.146650	.146613	.146590	.146734	.145060	.145087	.145536	.1501
16x16	.154149	.153775	.153765	.153752	.153801	.153419	.153406	.153478	.1553

Table 7.22: Skew cantilever plate - angle 60° mesh A - : displacement at node 2 ($\times Et^3/qL^4$)

Mesh	EL1R	EL1	EL2-A	EL2-B	EL2-C	EL3-A	EL3-B	EL3-C	DRM3
2x2	.367631	.290474	.283826	.249687	.296106	.155748	.170417	.171538	.8523
4x4	.518690	.477796	.474420	.462367	.480350	.310635	.323113	.324108	.7956
8x8	.662627	.652909	.652109	.651030	.653369	.574435	.577596	.578088	.7935
16x16	.763424	.761997	.761859	.761874	.762053	.745315	.745581	.745681	.8128

Table 7.23: Skew cantilever plate - angle 60° mesh B - : displacement of node 1 ($\times Et^3/qL^4$)

Mesh	EL1R	EL1	EL2-A	EL2-B	EL2-C	EL3-A	EL3-B	EL3-C	DRM3
2x2	.102517	.099400	.098642	.100262	.099487	.096536	.098428	.098972	.2133
4x4	.119029	.119028	.118866	.119611	.118998	.120757	.121090	.121201	.1551
8x8	.134256	.134310	.134289	.134402	.134303	.137780	.137696	.137722	.1437
16x16	.144779	.144725	.144722	.144721	.144727	.145721	.145705	.145715	.1471

Table 7.24: Skew cantilever plate - angle 60° mesh B - : displacement at node 2 ($\times Et^3/qL^4$)

7.7 Simply supported skew plate

This example is a highly skewed simply supported plate ($\beta = 60^{\circ}$). Two different thickness are considered. The plate properties are

$$E = 30E7 \ , \quad \nu = 0.3$$

with side length 100 and load 1.0.

Mesh	EL1R	EL1	EL2-A	EL2-B	EL2-C	EL3-A	EL3-B	EL3-C
3	2.87037	2.46210	2.39802	2.50654	2.47837	2.41092	2.46684	2.49180
5	3.38456	3.23114	3.18778	3.25044	3.23833	3.12517	3.20955	3.22440
9	3.71601	3.67143	3.65815	3.68645	3.67250	3.68221	3.71345	3.71970
17	4.01209	3.98147	3.97822	3.97702	3.98293	4.02540	4.02589	4.02870
33	4.23750	4.22402	4.22302	4.22226	4.22461	4.20739	4.20806	4.20921
Ref.[33]	4.455	4.455	4.455	4.455	4.455	4.455	4.455	4.455

Table 7.25: Simply supported skew plate - thickness t=1.0 - : displacement at the center ($\times 10^2$)

Mesh	EL1R	EL1	EL2-A	EL2-B	EL2-C	EL3-A	EL3-B	EL3-C
3	28.6480	24.5647	23.9207	25.0081	24.7267	24.0534	24.5914	24.8652
5	33.7681	32.1938	31.7060	32.2747	32.2718	30.0651	31.8535	32.0609
9	37.0388	36.6026	36.4167	36.6184	36.6088	33.7331	36.6316	36.7617
17	39.9055	39.5692	39.5538	39.2315	39.5797	37.4445	39.6949	39.7900
33	41.9923	41.6196	41.6147	41.2320	41.6474	40.6170	41.3902	41.4333
Ref.[33]	44.55	44.55	44.55	44.55	44.55	44.55	44.55	44.55

Table 7.26: Simply supported skew plate - thickness t=0.1 - : displacement at the center

CLOSURE

A set of three-node triangular elements for analysis of thick and thin plate bending problems has been presented. Each element has three external degrees-of-freedom at each vertex: a transverse displacement, w, and two rotations, θ_x and θ_y. Each element has been carefully analyzed with respect to the mixed patch test, as well as, on several test problems. While two of the elements are deficient in meeting proper rank conditions (on a single element only) one, EL1, is among the best for *all* numerical problems considered - especially when reduced quadrature is used to evaluate the transverse shear $\bar{\mathbf{B}}_s$ (EL1R).

In closing we note that all the elements considered may be easily extended to include non-linear constitutive or large displacement effects. They may also be incorporated into an adaptive mesh strategy using triangles as proposed by Zienkiewicz and Zhu [34,35]. Thus the elements provide a viable basis for general applications in plates and, when combined with a membrane element, to general shells.

REFERENCES

[1] R.H.Gallagher, "Finite element analysis fundamentals", Prentice Hall, Englewood Cliffs, N.J., 1975

[2] T.J.R Hughes, "The finite element method - linear static and dynamic finite element analysis", Prentice Hall, 1987

[3] R.D.Cook, D.S.Malkus and M.E.Plesha, "Concepts and applications of finite elements analysis", John Wiley & Sons, 3rd ed., 1989

[4] O.C.Zienkiewicz and R.L.Taylor, "The finite element method", McGraw Hill, New York, 4th ed., 1989, vol. I

[5] O.C.Zienkiewicz and R.L.Taylor, "The finite element method", McGraw Hill, New York, 4th ed., 1991, vol. II

[6] R.W.Clough and J.L.Tocher, "Finite element stiffness matrices for analysis of plate bending", Proc. Conf. on Matrix Methods in Structural Mechanics, Wright-Paterson Air Force Base, Ohio, October 1965

[7] G.P.Bazeley, Y.K.Cheung, B.M.Irons and O.C.Zienkiewicz, "Triangular elements in bending - conforming and non-conforming solution", Proc. Conf. on Matrix Methods in Structural Mechanics, Wright-Paterson Air Force Base, Ohio, October 1965

[8] G.A.Butlin and R.Ford, "A compatible triangular plate bending finite element", Int. J. Solids Structures, **6**, pp. 323-332, 1970

[9] E.Reissner, "The effect of transverse shear deformation on the bending of elastic plates", J. Appl. Mech., **12**, pp. 69-76, 1945

[10] R.D.Mindlin, "Influence of rotatory inertia and shear in flexural motion of isotropic, elastic plates", J. Appl. Mech., **18**, pp. 31-38,1951

[11] E.D.L.Pugh, E.Hinton and O.C.Zienkiewicz, "A study of quadrilateral plate bending elements with reduced integration", Int. J. Numer. Meth. Eng., **12**, pp. 1059-1079, 1977

[12] O.C.Zienkiewicz, J.Too and R.L.Taylor, "Reduced integration techniques in general analysis of plates and shells", Int. J. Numer. Meth. Eng., **3**, pp. 275-290, 1971

[13] T.J.R.Hughes, R.L.Taylor and W.Kanoknukulchai, "A simple and efficient element for plate bending", Int. J. Numer. Meth. Eng., **11**, pp. 1529-1543, 1977

[14] T.J.R.Hughes, M.Cohen and M.Haroun, "Reduced and selective integration techniques in the finite element analysis of plates", Nucl. Eng. Des., **46**, pp. 203-222, 1978

[15] D.S.Malkus and T.J.R.Hughes, "Mixed finite element methods - reduced and selective integration techniques: a unification of concepts', Comp. Methods Appl. Mech. Eng., **15**, pp. 63-81, 1978

[16] T.J.R.Hughes and M.Cohen, "The *heterosis* finite element for plate bending", Computers & Structure, **9**, pp. 445-450, 1978

[17] J.L.Batoz, K.J.Bathe and L.W.Ho, "A study of three node triangular plate bending elements", Int. J. Numer. Meth. Eng., **15**, pp. 1771-1812, 1980

[18] T.J.R.Hughes and T.E.Tezduyar, "Finite element based upon Mindlin plate theory with particular reference to the four node bilinear isoparametric element", Journal of Applied Mechanics, **48**, pp. 587-596, 1981

[19] M.M.Hrabok and T.M.Hrudey, "A review and catalogue of plate bending finite elements", Computers & Structures, 19, **3**, pp. 479-495, 1984

[20] K.J.Bathe and E.N.Dvorkin, "A four-node plate bending element based on Mindlin/Reissner plate theory and mixed interpolation", Int. J. Numer. Meth. Eng., **21**, pp. 367-383, 1985

[21] I.Babuska, "Error bounds for finite element methods", Num. Math., **16**, pp. 322-333, 1971

[22] I.Babuska, "The finite element method with Lagrange multipliers", Num. Math., **20**, pp. 179-192, 1973

[23] F.Brezzi, "On the existence, uniqueness and approximation of saddle point problems arising from Lagrange multipliers", RAIRO, **8**, pp. 129-151, 1971

[24] R.L.Taylor, J.C.Simo, O.C.Zienkiewicz and C.H.Chan, "The patch test - a condition for assessing fem convergence", Int. J. Numer. Meth. Eng., **22**, pp. 39-62, 1986

[25] O.C.Zienkiewicz, S.Qu, R.L.Taylor and S.Nakazawa, "The patch test for mixed formulation", Int. J. Numer. Meth. Eng., **23**, pp. 1873-1883, 1986

[26] O.C.Zienkiewicz and D.Lefebvre, "Three-field mixed approximation and the plate bending problem", Comm. Appl. Numer. Meth., **3**, pp. 301-309, 1987

[27] O.C.Zienkiewicz and D.Lefebvre, "Mixed methods for F.E.M. and the patch test: some recent development", Analyse Mathematique et Applications, Gauthier-Villars, Paris, 1988

[28] O.C.Zienkiewicz and D.Lefebvre, "A robust triangular plate bending element of Reissner-Mindlin type", Int. J. Numer. Meth. Eng., **26**, pp. 1169-1184, 1988

[29] O.C.Zienkiewicz, R.L.Taylor, P.Papadopoulos and E.Onate, "Plate bending elements with discrete constraints: new triangular elements", Computers & Structures, **35**, pp. 505-522, 1990

[30] P.Papadopoulos and R.L.Taylor, "A triangular element based on Reissner-Mindlin plate theory", Int. J. Numer. Meth. Eng., **30**, pp. 1029-1049, 1988

[31] Z.Xu, "A simple and efficient triangular finite element for plate bending", Acta Mechanica Sinica, **2**, vol.2, pp. 185-192, 1986

[32] S.Timoshenko and S.Woinowsky-Krieger, "Theory of plates and shells", McGraw Hill, New York, 1959

[33] L.S.D.Morley, "Skew plates and structures", Pergamon Press, 1963

[34] O.C.Zienkiewicz and J.Z.Zhu, "A simple error estimate and adaptive procedure for practical engineering analysis", Int. J. Numer. Meth. Eng., **24**, pp. 337-357, 1987

[35] J.Z.Zhu and O.C.Zienkiewicz, "Adaptive techniques in the finite element methods", Comm. Appl. Num. Math., **4**, pp. 197-204, 1988

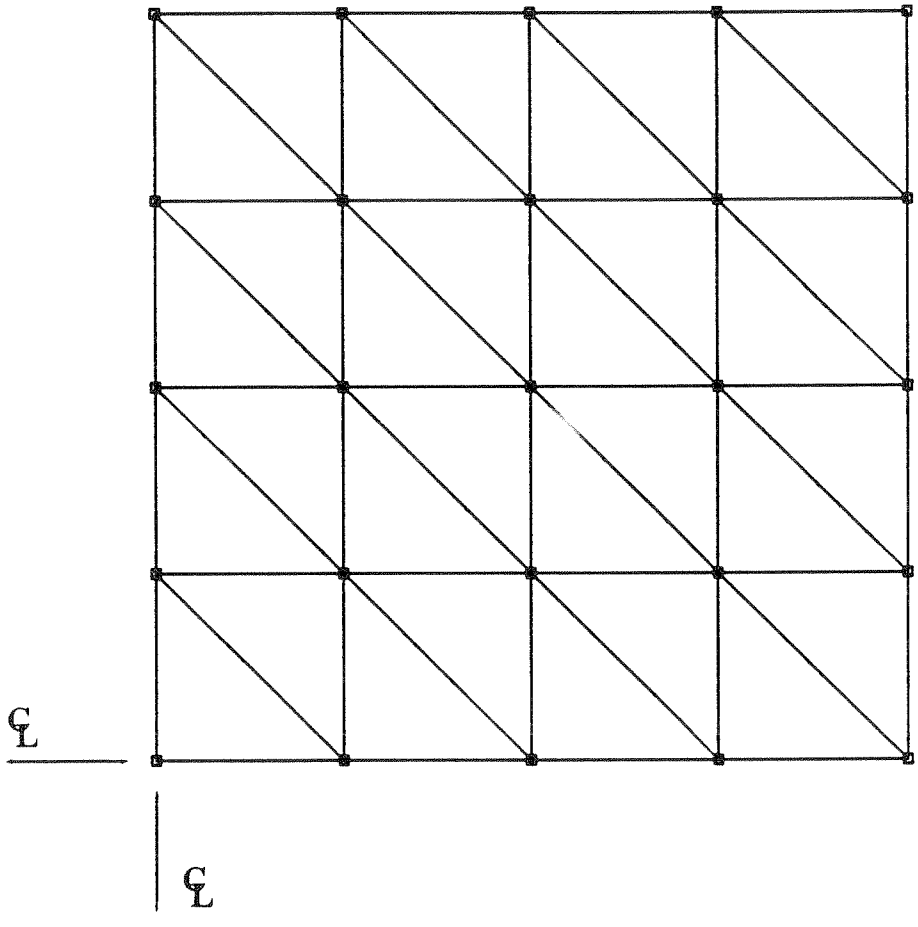

Fig.7.1A Square plate mesh: 8x8 elements, mesh type A

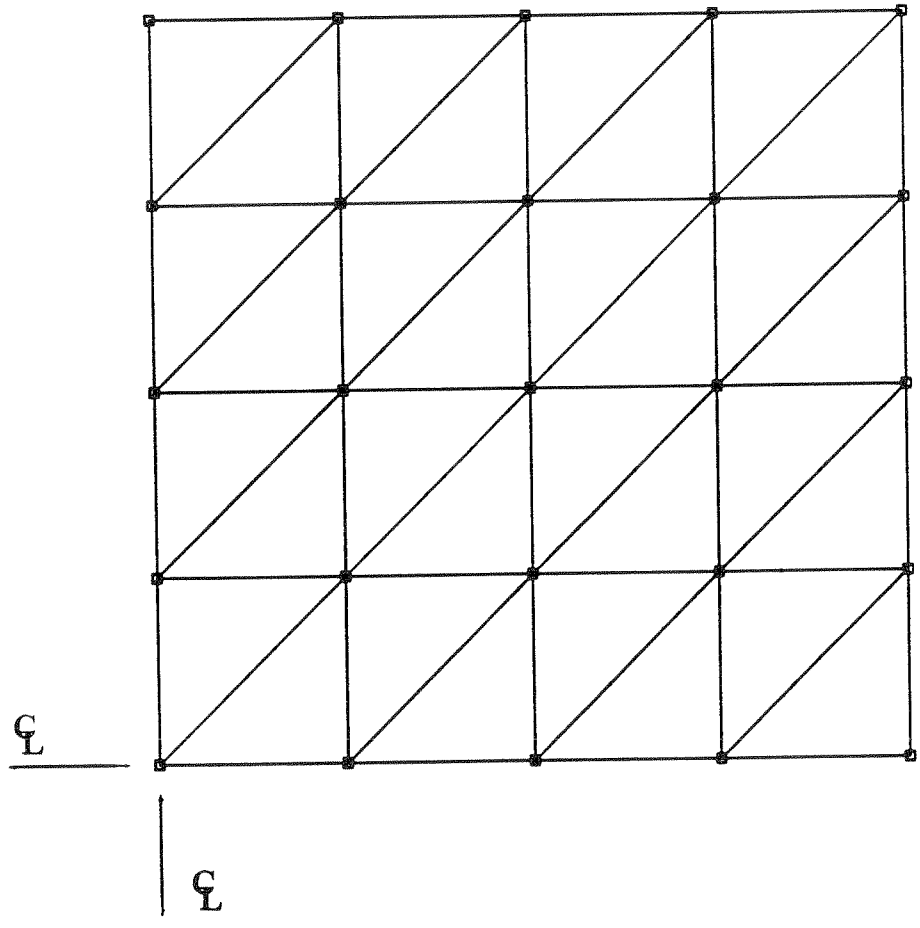

Fig.7.1B Square plate mesh: 8x8 elements, mesh type B

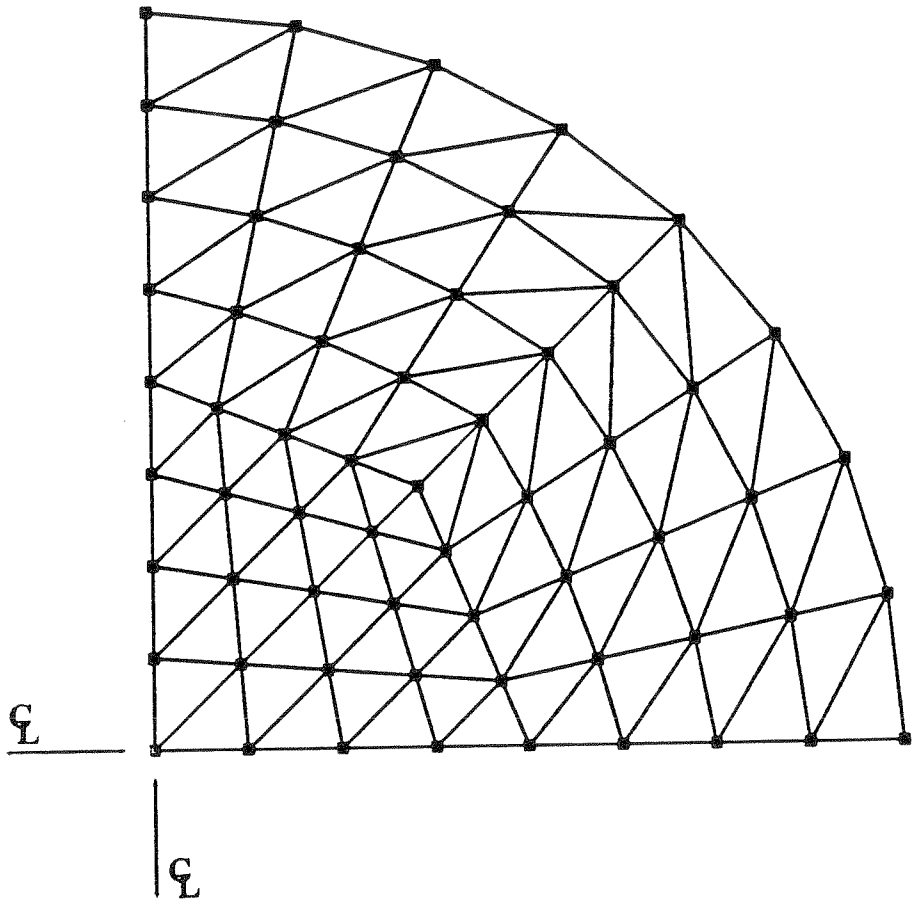

Fig.7.2 Circular plate mesh: 96 elements

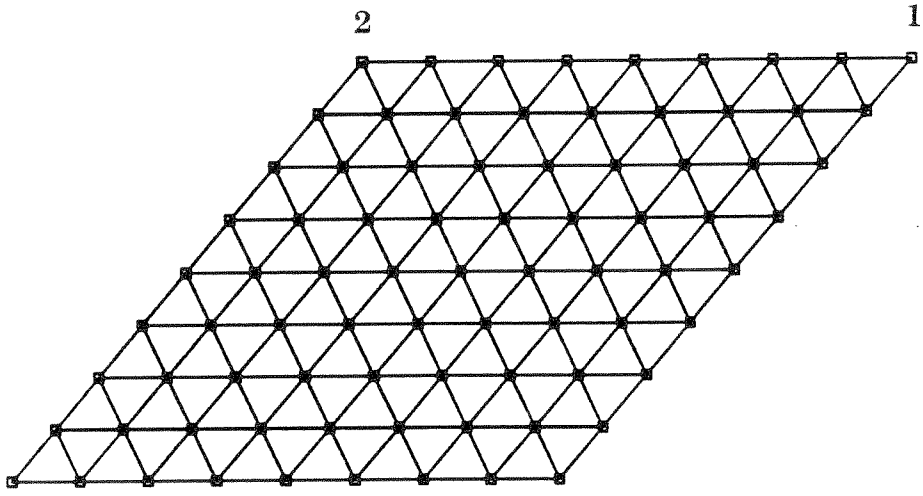

Fig.7.3 Skew cantilever plate: 8x8 elements, mesh type A, $\beta = 60^{\circ}$